CHINESE OPTICS LETTERS

Vol. 23, No. 1 | January 2025

Passively mode-locked Tm, La:CaF_2 crystal lasers near 1.9 μm water absorption band

Yuanhao Zhao (赵元昊)[1], Qianqian Hao (郝倩倩)[1,2], Zhen Zhang (张 振)[3], Jiahao Dong (董佳昊)[1], Luyang Tong (仝鲁阳)[1], Jingjing Liu (刘晶晶)[1], Lina Zhao (赵丽娜)[1], Jie Liu (刘 杰)[1*], and Liangbi Su (苏良碧)[3]

[1] Shandong Provincial Engineering and Technical Center of Light Manipulations & Shandong Provincial Key Laboratory of Optics and Photonic Devices, School of Physics and Electronics, Shandong Normal University, Jinan 250358, China

[2] Xinjiang Technical Institute of Physics and Chemistry, Chinese Academy of Sciences, Urumqi 830011, China

[3] State Key Laboratory of High Performance Ceramics and Superfine Microstructure, Shanghai Institute of Ceramics, Chinese Academy of Sciences, Shanghai 201899, China

*Corresponding author: jieliu@sdnu.edu.cn

Received April 29, 2024 | Accepted July 9, 2024 | Posted Online January 21, 2025

A diode-pumped mode-locked (ML) Tm,La:CaF_2 crystal laser is reported in this paper. This laser system delivers stable continuous-wave ML pulses, achieving a maximum output power of 143 mW at a fundamental frequency of 96.2 MHz. Moreover, the signal-to-noise ratio in the stabilized single-pulse regime reaches as high as 75 dB. The central wavelengths of the laser are located at 1886.5 and 1886.7 nm, which further advances the development of ultrafast lasers in the water absorption band of 1.8–1.9 μm.

Keywords: mode locking; LD pump; water absorption band; Tm,La:CaF_2 crystal.
DOI: 10.3788/COL202523.011401

1. Introduction

Mode-locked (ML) lasers around 2 μm with pulse widths in the picosecond and femtosecond orders have been used in applications, such as remote detection radar systems, eye laser minimally invasive surgery, gas detection, and material micromachining[1–4]. Relevant literature indicates that pulse durations in the picosecond range are advantageous for precision micromachining. Additionally, they can yield high average power and beam quality, thereby qualifying micromachining technology for industrial applications[5,6].

The 1.8–1.9 μm band intersects with the absorption peak of water[7], impacting the stability of continuous-wave mode-locked (CWML) lasers. This interference induces dispersion in the laser spectra, resulting in the broadening of the pulse width[8]. If progress is to be made in the direction of ultrafast lasers in this band, Tm^{3+}-doped lasers need more in-depth exploration and new experimentation. The strong absorption band of Tm^{3+} ion is around 800 nm, exactly coinciding with the wavelength of the commercial AlGaAs laser diode (LD), which makes the structure of the laser system simple, efficient, and more conducive to the realization of commercialization. Currently, Tm^{3+} ultrafast solid-state lasers at wavelengths exceeding 2 μm have been advanced to pulse widths below 100 fs[9–15], whereas ultrafast lasers near 1.9 μm are lagging due to the significant water absorption[16–20], despite their importance in practical applications. Therefore, achieving stable mode-locking within the water absorption band remains a significant challenge, awaiting further development and maturation.

The existing Tm^{3+}-doped gain media suitable for ultrafast lasers have been studied deeply in recent years. Compared to other monocrystalline hosts available, calcium fluoride (CaF_2) crystals, which can be commercialized for large-size growth, have low photon energy (322 cm^{-1}), which leads to the favorable phenomenon that cluster structure can be formed even at low doping concentration levels of rare earth ions[21]. Within the cubic lattice structure of CaF_2, F^- compensating ions are positioned in the corners of the cubic structure, while Ca^{2+} ions are positioned in the center. Clusters to a certain extent facilitate the improvement of gain medium laser characteristics. In Tm^{3+} clusters, energy transfer between adjacent ions results in cross-relaxation processes, where one Tm^{3+} ion in the ground state transitions to the excited state, thereby enhancing pump efficiency. The cross-relaxation of heavily doped crystals can completely suppress 1.5 μm fluorescence. Although the cluster effect formed by high Tm^{3+} doping can enhance crystal performance, higher Tm^{3+} concentrations do not necessarily equate to better performance. With increasing Tm^{3+} doping concentration, ions in the laser upper level undergo reverse cross-relaxation, leading to photon quenching. Additionally, heavily doped

crystals generate a large number of defects during growth, which also contribute to laser quenching. When doped with Tm^{3+} and La^{3+} ions, these two ions and F^- ions will take up the space of the lattice at random, and co-doped crystals exhibit fewer clusters and defects compared to singly doped crystals, leading to the formation of a disordered lattice field, then ground state splitting and spectral broadening[19,22]. Observing its spectral morphology can provide insights into the material's potential for mode-locking to some extent. Combined with the above theory, we select Tm, La:CaF_2 single crystal with appropriate doping concentration as the gain medium to study its performance in mode-locking.

Zhang *et al.* in 2018 successfully verified the highly efficient laser output of Tm, La:CaF_2 single crystal, achieving a slope efficiency of nearly twice the theoretical quantum efficiency and a tunable spectral range as wide as 192 nm[23]. Then, the passively and actively *Q*-switched Tm, La:CaF_2 lasers were likewise successfully obtained separately by Zu *et al.* in 2019[24] and Hao *et al.* in 2022[25]. However, the CWML operation of Tm, La:CaF_2 single crystal has not been reported yet. The possibility of Tm, La:CaF_2 single crystal for the generation of ultrashort pulses with high repetition frequency needs to be exploited.

In this paper, we report, to the best of our knowledge, the first demonstration of a highly stable CWML Tm, La:CaF_2 laser. The initial investigation was conducted in the continuous-wave (CW) regime, achieving a maximum output power of 427 mW at an absorbed pump power of 2.26 W with a slope efficiency of 20.4%. A self-starting passively CWML laser was subsequently obtained at 1886.5 and 1886.7 nm, exhibiting a significantly high extinction ratio of 75 dB. The laser generated a smooth pulse train with a pulse duration of 284.8 ps and a maximum average output power of 143 mW.

2. Experimental Setup and Discussion

We designed a tightly focusing five-mirror X-shaped cavity, as illustrated in Fig. 1, to ensure the appropriate energy density to support the stable operation of CWML. The gain medium selected for this experiment was a 5.5-mm-thick 3% (atomic fraction) Tm^{3+} and 2% (atomic fraction) La^{3+} co-doped disordered CaF_2 crystal with the cross-section size of 3 mm × 3 mm, grown by the temperature gradient method. Both sides of the crystal were plated with anti-reflection (AR) films for 792 and 1780–1980 nm in order to reduce Fresnel reflection loss. The single crystal, tightly mounted in a copper block, was water-cooled to maintain 12°C to mitigate the thermal load. The room temperature absorption and emission spectra of Tm, La:CaF_2 crystal were demonstrated in our previous work[23]. There is a strong absorption band at 792 nm corresponding to the $^3H_6 - {}^3H_4$ energy level transition of Tm^{3+} ion. The pumping source was a fiber-coupled LD with a wavelength of 792 nm, a numerical aperture of 0.22, and a core diameter of 105 μm. The pumping laser was focused into the crystal through a collimation system with a focusing ratio of 1:1, ensuring the attainment of the appropriate mode volume. The absorption of the incident pump power by the Tm, La:CaF_2 sample was about 30%.

When the oscillator worked in the CW state, the input mirror (M_1) (R = −100 mm) and other mirrors ($M_2 - M_4$) (M_2:R = −200 mm, M_3:R = −100 mm, and M_4:R = ∞) were all AR coated at 780–810 nm and high-reflection (HR) coated at 1900–2000 nm. The output mirror (M_5) was a plane mirror with the transmission of 2% for the oscillating laser. The CW laser output performance of the Tm, La:CaF_2 crystal was shown in Fig. 2. The laser threshold was observed to be low when the absorbed pump power reached 160 mW and the slope efficiency was about 20.4%. When the absorbed pump power reached 2.26 W, the maximum output power was 427 mW, with optical-to-optical efficiency of 18.9%, at which point laser saturation was approached. The CW laser spectrum, centered at 1886.2 and 1886.5 nm, was scanned using an optical spectrum analyzer (MS3504i), as depicted in Fig. 3(a). The spectrum showed a narrow and double-peak structure mainly due to the inhomogeneous spectral splitting in the disordered crystals, the influence of water molecules, and the imperfect stability of the coating process.

To investigate the performance of the CWML, the semiconductor saturable absorber mirror (SESAM) (BATOP GmbH, SAM-1920-2-30 ps-4.0-25.4s-e) served as an excellent replacement for M_4, positioned at the second beam waist generated by M_3. The resonator length and mode of the laser will affect pulse characteristics. The length of the gain medium, one of the influencing factors, can impact the optical path length of

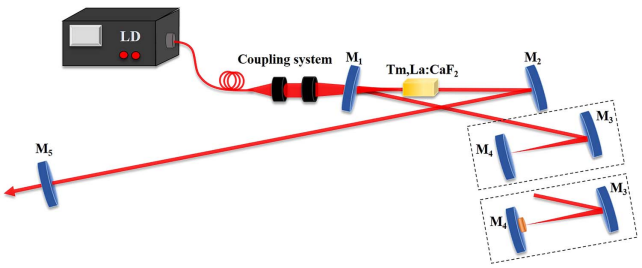

Fig. 1. Schematic of the CW and CWML Tm,La:CaF_2 lasers.

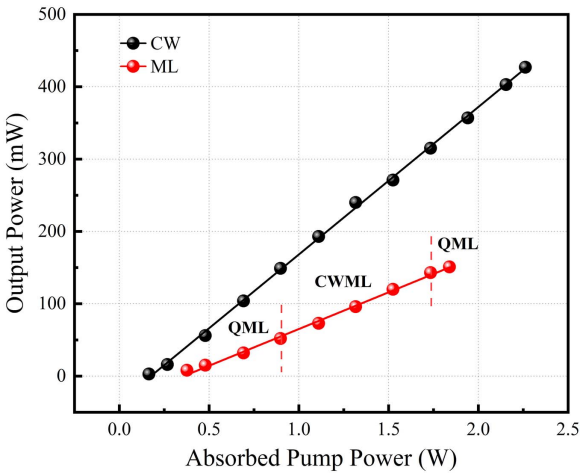

Fig. 2. Average output power as a function of the pump power.

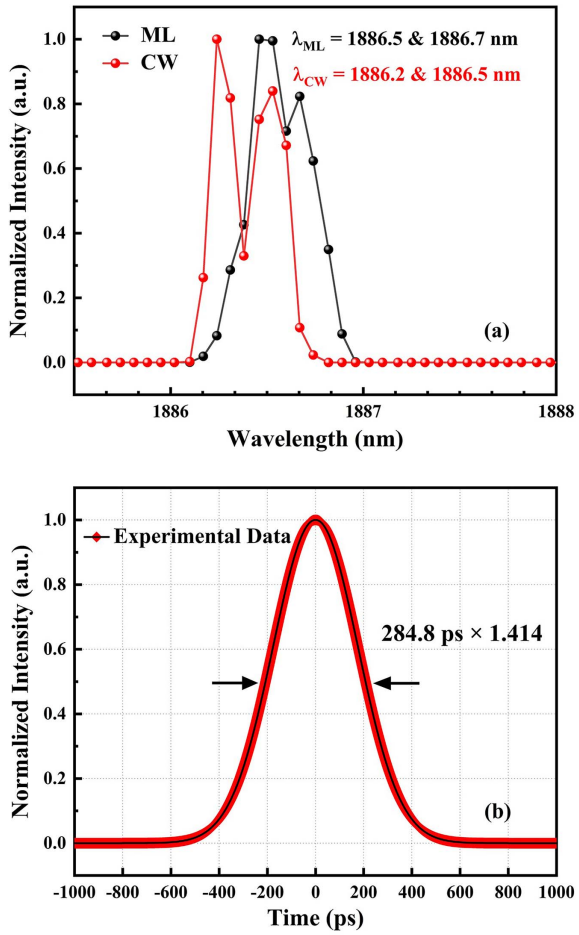

Fig. 3. (a) Laser emission spectra of CW and CWML Tm,La:CaF_2 lasers. (b) Intensity autocorrelation trace.

the resonator, thereby affecting the laser's mode and pulse frequency. By computing and simulating the relationship between the crystal length and cavity modes, the optimal cavity length for achieving the desired pulse state is determined. The total physical length of the cavity was 1.56 m, and the mode radius at the single crystal and the SESAM were calculated to be ~56 and ~34.5 μm. Simultaneously, the small laser pattern facilitates low-threshold laser operation.

When the absorption of pump power exceeded 0.9 W, the unstable *Q*-switched ML state transitioned into a CWML state, with a minimum output power of 52 mW. Once established, the CWML state could restart itself each time without the need for adjustment and remained continuous for hours in the absence of external interference. As Fig. 2 illustrates, the maximum average output power of 143 mW and pulse energy of 1.5 nJ at 96.2 MHz pulse repetition frequency were obtained under an absorbed pump power of 1.73 W, corresponding to the maximum average fluence (I_{max}) of 3.94 mJ/cm^2 on the SESAM. Imax can be estimated by the following equation:

$$I_{max} = \frac{P_{max}}{f} \cdot \frac{1 + R_{OC}}{1 - R_{OC}} \cdot \frac{1}{A_{eff,A}}, \quad (1)$$

where P_{max}, f, R_{oc}, and $A_{eff,A}$ are the maximum output power, repetition frequency, reflectivity of the output mirror, and effective laser mode area on the SESAM. The damage threshold of the SESAM is 4 mJ/cm^2, which is very close to I_{max}. Keeping on increasing the incident pump power, the CWML state will be destabilized and revert to the *Q*-switched ML state. At this point, a hasty increase of power is most likely to lead to damage to the SESAM. In subsequent research, to surpass the current maximum output power, options such as adjusting the spot size at the SESAM to increase its size moderately or exploring ML elements with higher damage thresholds may be considered.

As can be seen from Fig. 3, the CWML optical spectrum and autocorrelation trace were detected. It was observed that the output spectrum under the CWML state still owned double central peaks, with a slight red shift to 1886.5 and 1886.7 nm. Although a spectral broadening phenomenon was observed, it became less prominent after data processing. The essential parameter, pulse width, was measured by a high dynamic range autocorrelator (A.P.E. GmbH, pulseCheck SM). By assuming a Gaussian-fit envelope profile, the pulse duration was found to be 284.8 ps. The corresponding time-bandwidth product was calculated to be 9.6. The wide pulse width obtained is mainly limited by several aspects. First, dispersion compensation is not applied to the cavity. Second, the SESAM has a small saturable fluence (45 μJ/cm^2) and a slow recovery time (30 ps). The shorter the recovery time is, the narrower the CWML pulse width that can be obtained[26]. In addition, the output wavelength is centered at ~1886 nm, which will be directly impacted by the humidity of the ultra-clean room, especially during the summer rainy season. Meantime, the band is at the edge of the SESAM's high-reflection band (1880–1980 nm), creating a huge obstacle in realizing wide-band ultrafast mode-locking. Hence, it is anticipated that the pulse width of the Tm, La:CaF_2 single crystal could be significantly reduced through the preparation of more parameterized SESAM devices, combined with a more proficient technical approach by experimentalists.

Using the 90/10 knife-edge method, we analyzed the diffracted beam quality in the two orthogonal directions (M_x^2 = 1.42, M_y^2 = 1.43), shown in Fig. 4. The ML beam profile and 3D intensity distribution were measured by a mid-infrared broadband phasor-type beam quality analyzer (WinCamD-IR-BB, 2–16 μm, USA), as shown in the inset of Fig. 4. Under the combination of the astigmatism of multiple cavity mirrors and the presence of measurement errors that cannot be ruled out, M^2 factors showed only slight differences in x and y directions.

Thereafter, to evaluate the stability of the CWML laser, the temporal waveforms of real-time pulse trains were recorded and monitored by a high-speed photodetector (EOT, ER-5000, rise/fall time of 28 ps, > 110 GHz) and a digital oscilloscope (Tektronix DPO4104, 1 GHz), as displayed in Fig. 5(a). The good pulse-to-pulse stability of the CWML laser was evidenced by the clean individual pulse at nanosecond time scale as well as the smooth and neat periodic pulse sequences over 20 ms/div wide time scale. To further verify the high stability of the

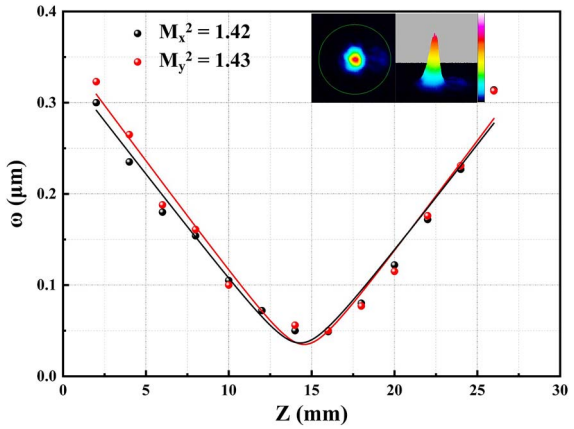

Fig. 4. M^2 factors of the CWML laser. The inset shows the measured beam profile and 3D intensity distribution.

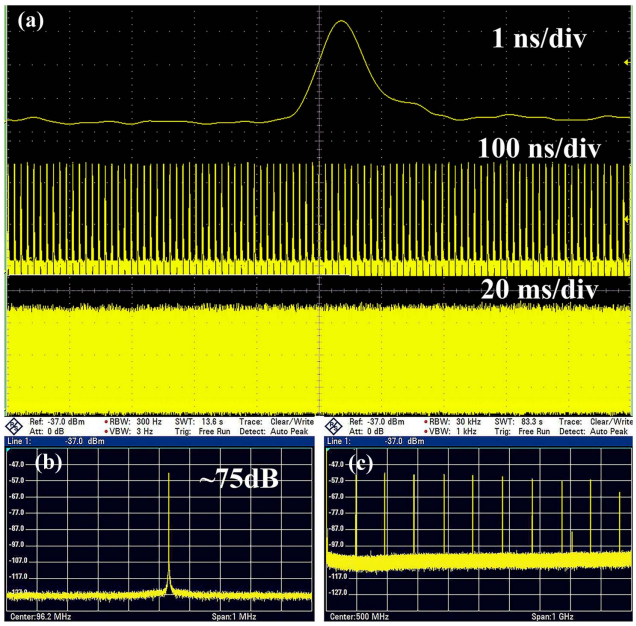

Fig. 5. (a) Temporal traces of CWML Tm, La:CaF_2 pulses in different time scales. RFS in stabilized single-pulse regime: (b) fundamental beat note, RBW = 300 Hz; (c) its harmonics in 1 GHz frequency windows, RBW = 30 kHz. RBW: resolution bandwidth.

CWML laser, a spectrum analyzer (ROHDE & SCHWARZ-FSC) was selected to measure the radio frequency spectrum (RFS) and signal-to-noise ratio (SNR). As the lab results showed, the clean fundamental peak at 96.2 MHz without side peaks was in perfect agreement with the round-trip time of the cavity, demonstrating an excellent CWML state without the accompanying *Q*-switched instability. The SNR was up to 75 dB, indicating a pure mode-locking with a minimal CW component present. In addition, the single-frequency ML state had also been confirmed by the comb-like spectrum at a broad scan range (1 GHz), as depicted in Fig. 5(c). All of the aforementioned observations indicate that we have achieved a CWML laser characterized by extremely high stability in pulse energy fluctuation at the nearly 1.9 μm wavelength band. This is crucial for applications requiring ultrashort lasers within the 1.8–1.9 μm spectral window.

3. Conclusion

In conclusion, the first CWML Tm, La:CaF_2 laser has been demonstrated, to the best of our knowledge. For the CW mode, the maximum output power was 427 mW with 20.4% slope efficiency. By replacing the end mirror with a SESAM, we obtained a highly stable CWML laser, delivering a laser pulse with 284.8 ps width at wavelengths of 1886.5 and 1886.7 nm. The SNR is up to 75 dB, which can represent a prominent level available in LD-pumped crystalline single-doped Tm^{3+} CWML lasers under the fundamental frequency of 96.2 MHz. We have succeeded in making Tm, La:CaF_2 lasers capable of realizing high-frequency mode-locking in the picosecond scale in the band of 1.9 μm.

Acknowledgements

This work was supported by the National Natural Science Foundation of China (Nos. 11974220 and 12374401).

References

1. M. Li, Y. Song, C. Zhang, *et al.*, "Generation and observation of multiple solitons from a mid-infrared ultrafast fiber laser," Chin. Opt. Lett. **22**, 031405 (2024).
2. A. Godard, "Infrared (2–12 μm) solid-state laser sources: a review," C.R. Phys. **8**, 1100 (2007).
3. F. M. P. Leclère, M. Schoofs, F. Auger, *et al.*, "Blood flow assessment with magnetic resonance imaging after 1.9 μm diode laser-assisted microvascular anastomosis," Lasers Surg. Med. **42**, 299 (2010).
4. W. Y. He, P. Yao, D. K. Chu, *et al.*, "Fabrication and cell-adhesion evaluation of laser-ablated microprotrusion or microgroove on titanium," Chin. J. Lasers **49**, 1002605 (2022).
5. C. Foehl, D. Breitling, K. Jasper, *et al.*, "Precision drilling of metals and ceramics with short- and ultrashort-pulsed solid state lasers," in *International Symposium on Laser Precision Microfabrication* (2002).
6. A. Ostendorf and F. Siegel, "Micro-machining using high energy picosecond laser pulses a cause-effect consideration," in *ICALEO 2004 - 23rd International Congress on Applications of Laser and Electro-Optics, Congress Proceedings* (2004).
7. G. M. Hale and M. R. Querry, "Optical constants of water in the 200-nm to 200-μm wavelength region," Appl. Opt. **12**, 555 (1973).
8. X. Cao, Q. Zhu, A. Xian, *et al.*, "Ultrafast Tm:$CaYAlO_4$ laser with pulse regulation and saturation parameters evolution in the 2 μm water absorption band," Opt. Laser Technol. **152**, 108096 (2022).
9. Y. Wang, W. Jing, P. Loiko, *et al.*, "Sub-10 optical-cycle passively mode-locked Tm:$(Lu_{2/3}Sc_{1/3})_2O_3$ ceramic laser at 2 μm," Opt. Express **26**, 10299 (2018).
10. Y. Zhao, L. Wang, W. Chen, *et al.*, "SESAM mode-locked Tm:$LuYO_3$ ceramic laser generating 54-fs pulses at 2048 nm," Appl. Opt. **59**, 10493 (2020).
11. Z. Pan, Y. Wang, Y. Zhao, *et al.*, "Generation of 84-fs pulses from a mode-locked Tm:CNNGG disordered garnet crystal laser," Photonics Res. **6**, 800 (2018).
12. L. Dong, N. Zhang, H. Ding, *et al.*, "Femtosecond pulse generation from a Tm:$CaYLuAlO_4$ laser employing a birefringent filter as wavelength selector," Appl. Phys. B **129**, 114 (2023).

13. N. Zhang, Z. Wang, S. Liu, *et al.*, "Watt-level femtosecond Tm-doped 'mixed' sesquioxide ceramic laser in-band pumped by a Raman fiber laser at 1627 nm," Opt. Express **30**, 23978 (2022).
14. A. A. Lagatsky, S. Calvez, J. A. Gupta, *et al.*, "Broadly tunable femtosecond mode-locking in a Tm:KYW laser near 2 μm," Opt. Express **19**, 9995 (2011).
15. A. Suzuki, S. Kalusniak, S. Ganschow, *et al.*, "Kerr-lens mode-locked 49-fs Tm^{3+}:$YScO_3$ single-crystal laser at 2.1 μm," Opt. Lett. **48**, 4221 (2023).
16. Q. Na, Z. Huang, M. He, *et al.*, "Watt-level passively mode-locked Tm:YLF laser at 1.83 μm," Opt. Express **27**, 35230 (2019).
17. W. Zhou, X. Xu, R. Xu, *et al.*, "Watt-level broadly wavelength tunable mode-locked solid-state laser in the 2 μm water absorption region," Photonics Res. **5**, 583 (2017).
18. Q. Na, C. Xu, H. Chen, *et al.*, "Continuous-wave and mode-locking operation of Tm:YAP lasers near 1.8 μm," Opt. Laser Technol. **142**, 107225 (2021).
19. L. Kong, Z. Qiao, G. Xie, *et al.*, "Spectroscopic characteristics, continuous-wave and mode-locking laser performances of Tm,Y:CaF_2 disordered crystal," Opt. Express **25**, 21267 (2017).
20. X. Zou, Y. Leng, Y. Li, *et al.*, "Passively Q-switched mode-locked Tm:LLF laser with a MoS_2 saturable absorber," Chin. Opt. Lett. **13**, 081405 (2015).
21. H. Wang, J. Zhu, Z. Gao, *et al.*, "Femtosecond mode-locked Nd,La:CaF_2 disordered crystal laser," Opt. Mater. Express **6**, 2184 (2016).
22. M. A. Hughes, M. A. Lourenço, J. D. Carey, *et al.*, "Crystal field analysis of Dy and Tm implanted silicon for photonic and quantum technologies," Opt. Express **22**, 29292 (2014).
23. Z. Zhang, X. Guo, J. Wang, *et al.*, "High-efficiency 2 μm continuous-wave laser in laser diode-pumped Tm^{3+}, La^{3+}: CaF_2 single crystal," Opt. Lett. **43**, 4300 (2018).
24. Y. Zu, X. Guo, J. Liu, *et al.*, "Passively Q-switched operation of a novel Tm^{3+}, La^{3+} co-doped CaF_2 single crystal near 2 μm," Infrared Phys. Technol. **102**, 103010 (2019).
25. Q. Hao, W. Liu, Y. Zu, *et al.*, "Highly efficient dual-wavelength acousto-optically Q-switched Tm,La:CaF_2 laser," Chin. Opt. Lett. **20**, 111402 (2022).
26. R. Paschotta and U. Keller, "Passive mode locking with slow saturable absorbers," Appl. Phys. B **73**, 653 (2001).